



NASA  
Technical Memorandum 100939

AVSCOM  
Technical Memorandum 88-C-004

# Applications of an Exponential Finite Difference Technique

AD-A199 197

Robert F. Handschuh  
*Propulsion Directorate*  
*U.S. Army Aviation Research and Technology Activity—AVSCOM*  
*Lewis Research Center*  
*Cleveland, Ohio*

and

Theo G. Keith, Jr.  
*University of Toledo*  
*Toledo, Ohio*

July 1988

DTIC  
ELECTE  
SEP 23 1988  
S H D



US ARMY  
AVIATION  
SYSTEMS COMMAND  
AVIATION R&T ACTIVITY

DISTRIBUTION STATEMENT A  
Approved for public release;  
Distribution Unlimited

88 9 22 035

## APPLICATIONS OF AN EXPONENTIAL FINITE DIFFERENCE TECHNIQUE

Robert F. Handschuh  
Propulsion Directorate  
U.S. Army Aviation Research and Technology Activity - AVSCOM  
Lewis Research Center  
Cleveland, Ohio 44135

and

Theo G. Keith, Jr.  
Department of Mechanical Engineering  
University of Toledo  
Toledo, Ohio 43606

### SUMMARY

An exponential finite difference scheme first presented by Bhattacharya for one-dimensional unsteady heat conduction problems in Cartesian coordinates has been extended. The finite difference algorithm developed was used to solve the unsteady diffusion equation in one-dimensional cylindrical coordinates and was applied to two- and three-dimensional conduction problems in Cartesian coordinates. Heat conduction involving variable thermal conductivity was also investigated. The method was used to solve nonlinear partial differential equations in one- (Burger's equation) and two- (boundary layer equations) dimensional Cartesian coordinates. Predicted results are compared to exact solutions where available or to results obtained by other numerical methods.

### INTRODUCTION

The objective of this work is to extend, expand, and compare an explicit exponential finite difference technique first proposed by Bhattacharya (ref. 1). To date the method has only been used for one-dimensional unsteady heat transfer in Cartesian coordinates. The method is a finite difference relative of the separation of variables technique. The finite difference equation that results uses time step division to increase accuracy and to maintain stability.

Following his initial paper, Bhattacharya (ref. 2) and Bhattacharya and Davies (ref. 3) have developed refined forms of the exponential finite difference equation. Also, an approximate substitution for a given range of exponential term was investigated to reduce the computation time while retaining good accuracy. In references 1 to 3, the results for unsteady one-dimensional heat transfer found by implicit and explicit numerical techniques were compared to exact analysis. The overall results indicated that the exponential finite difference techniques were more accurate than the other available numerical techniques. The one drawback with the exponential finite difference method was that computer time increased for the one-dimensional case that was investigated.

The intent of the present work is to demonstrate how the exponential finite difference method originally developed in reference 1 can be used to

solve a wide variety of problems. Linear and nonlinear partial differential equations found in engineering and physics will be solved. All results obtained by this finite difference technique will be compared to exact solutions or to values found by use of other numerical techniques.

#### NOMENCLATURE

B	Biot modulus, $hR/k$
$C_p$	material specific heat, $J/(kg)(K)$ ; $Btu/(lb_m)(^{\circ}F)$
h	convection heat transfer coefficient, $W/(m^2)(^{\circ}C)$ ; $Btu/(ft^2)(hr)(^{\circ}F)$
i,j,k	nodal location in x, y, and z spatial coordinate directions, respectively
$J_0, J_1$	Bessel functions of zero and first order, respectively
k	thermal conductivity, $W/(m)(^{\circ}C)$ ; $Btu/(hr)(^{\circ}F)(ft)$
$k_i^n$	thermal conductivity at $i^{th}$ position, $n^{th}$ time step, $W/(m)(^{\circ}C)$ ; $Btu/(hr)(^{\circ}F)(ft)$
L	distance between plates, m; ft
M	dimensionless drive number
m	number of subintervals
N	number of nodes in a spatial direction
n	time step position designation
$R, R_1, R_2$	radial length, m; ft
r	spatial coordinate (cylindrical coordinates), m; ft
T	temperature, $^{\circ}C$ ; $^{\circ}F$
t	time, s
$\Delta t$	time between time steps n and n + 1
U	flow velocity, m/s; ft/s
$\bar{U}, \bar{V}$	method of Douglas intermediate values
$\bar{\bar{U}}$	substitution variable for Burger's equation
x,y,z	spatial coordinates (Cartesian coordinates), m; ft
$\Delta x, \Delta y, \Delta z$	distance between nodal positions in the x, y, and z spatial directions, respectively



The spatial and temporal variables can be separated and equation (2) can then be set equal to a constant, say,  $-\kappa$ . Thus, the left side of equation (2) is written as

$$\left. \frac{\partial \ln T}{\partial t} \right|_{i,j}^n = -\kappa$$

Replacing the derivative with a one-sided difference results in the following:

$$\frac{\ln T_{i,j}^{n+1} - \ln T_{i,j}^n}{\Delta t} = -\kappa$$

or

$$\frac{T_{i,j}^{n+1}}{T_{i,j}^n} = e^{-\kappa \Delta t} \quad (3)$$

The separation constant  $\kappa$  is evaluated from the right side of equation (2) by using second central space differences which result in

$$-\kappa = \left[ \frac{\alpha}{T} \left( \frac{\partial^2 T}{\partial x^2} + \frac{\partial^2 T}{\partial y^2} \right) \right]_{i,j}^n = \frac{\alpha}{T_{i,j}^n} \left( \frac{T_{i+1,j}^n + T_{i-1,j}^n - 2T_{i,j}^n}{\Delta x^2} + \frac{T_{i,j+1}^n + T_{i,j-1}^n - 2T_{i,j}^n}{\Delta y^2} \right) \quad (4)$$

If the grid spacing is constant ( $\Delta x = \Delta y$ ), then equation (3) may be written as

$$\frac{T_{i,j}^{n+1}}{T_{i,j}^n} = e^{\Omega M_{i,j}^n} \quad (5)$$

where  $\Omega = \text{grid Fourier number} = (\alpha \Delta t) / \Delta x^2$  and  $M_{i,j}^n = \text{dimensionless drive number which is written as}$

$$M_{i,j}^n = \frac{T_{i+1,j}^n + T_{i-1,j}^n + T_{i,j+1}^n + T_{i,j-1}^n - 4T_{i,j}^n}{T_{i,j}^n} \quad (6)$$

Because of the exponential form of equation (5), the time step may be divided into a number of subintervals. Subdivisions or reduction of the time step is typically done to increase the accuracy of explicit numerical methods. For example, if the time step were divided into two intervals, then  $T_{i,j}^{n+1}$  would be found in the following way:

$$T_{i,j}^{n+1/3} = T_{i,j}^n \exp \left[ \frac{\Omega}{3} (M_{i,j}^n) \right]$$

$$T_{i,j}^{n+2/3} = T_{i,j}^{n+1/3} \exp\left[\frac{\Omega}{3} (M_{i,j}^{n+1/3})\right]$$

$$T_{i,j}^{n+1} = T_{i,j}^{n+2/3} \exp\left[\frac{\Omega}{3} (M_{i,j}^{n+2/3})\right]$$

Consequently,

$$T_{i,j}^{n+1} = T_{i,j}^n \exp\left[\frac{\Omega}{3} (M_{i,j}^n + M_{i,j}^{n+1/3} + M_{i,j}^{n+2/3})\right]$$

where the dimensionless drive numbers are evaluated at the sub-time intervals and then summed for calculation of "T" at the  $n + 1$  time step. Or in a more general form, for "m" subintervals

$$T_{i,j}^{n+1} = T_{i,j}^n \exp\left[\frac{\Omega}{m+1} \sum_{p=0}^m M_{i,j}^{n+p/(m+1)}\right] \quad (7)$$

Equation (7) is the general difference equation for the temperature at the  $i, j$  node, at the  $n + 1$  time step, for  $m$  time-step subintervals. This equation is valid for all interior nodes for two-dimensional rectangular domain. Nodes on the boundaries are treated differently and depend on the application.

In reference 1, it was shown that for heat transfer applications the time step can be subdivided to a maximum number of time subintervals as follows:

$$m = \begin{cases} (N/2) - 1 \rightarrow \text{heat transfer coefficient} \approx \text{infinite} \\ (N/2) + 1 \rightarrow \text{heat transfer coefficient finite} \end{cases} \quad (8)$$

where  $N$  equals the number of nodes in one of the coordinate directions.

#### STABILITY OF THE EXPONENTIAL FINITE DIFFERENCE METHOD

With few exceptions, explicit finite difference procedures for solving partial differential equations are inherently unstable unless certain numerical conditions are satisfied. These conditions take the form of a grid size and/or time step requirement written in terms of parameters of the given problem. If these stability conditions are not met, the solution can diverge. These constraints on grid size or length of time step can make the methods impractical for certain applications. These conditions, however, must be known prior to use of any explicit differencing procedure.

There are a variety of methods that have been used to establish the stability constraints of a finite difference procedure. These methods seek to find an expression for the amplification factor which is defined as the ratio of the current solution result to that in the previous step. If the absolute value of the ratio is less than one, then the method is regarded as being stable. Determination of the amplification factor for the exponential finite difference method is particularly convenient, as has been shown in reference 1. For the two-dimensional Cartesian coordinate case, the amplification factor  $\xi$  can be defined as the following (no time subinterval division):

$$\xi = \frac{T_{i,j}^{n+1}}{T_{i,j}^n} = \exp[\Omega(M_{i,j}^n)] \quad (9)$$

Numerical stability constraints require that

$$\lim_{\substack{\Delta t \rightarrow 0 \\ \Delta x \rightarrow 0}} |\xi| \leq 1 \quad (10)$$

To satisfy this requirement, the exponent of equation (9) must obviously be less than or equal to zero. Since the components that make up  $\Omega$  in that exponent are all positive, this implies that the dimensionless drive number will determine the numerical stability. For the two-dimensional Cartesian coordinate case the dimensionless drive number must satisfy

$$M_{i,j}^n = \frac{T_{i+1,j}^n + T_{i-1,j}^n + T_{i,j+1}^n + T_{i,j-1}^n - 4T_{i,j}^n}{T_{i,j}^n} \leq 0 \quad (11)$$

or

$$T_{i,j}^n \geq \frac{T_{i+1,j}^n + T_{i-1,j}^n + T_{i,j+1}^n + T_{i,j-1}^n}{4} \quad (12)$$

Equation (12) needs to be satisfied otherwise an unstable condition can exist. As pointed out by Bhattacharya (ref. 1), the dimensionless drive number primarily determines the stability of the solution. However a large dimensionless time step could also cause the solution to become unstable. Since time subinterval division is used, the total dimensionless time step  $\Omega$  could become quite large. In reference 1, it was recommended for one-dimensional heat conduction problems that the dimensionless time step satisfy the following condition:

$$\frac{\Omega}{m+1} \leq 0.5 \quad (13)$$

where  $m$  is the number of time-step subintervals involved in the calculations. This same reasoning can be extended to heat conduction problems in two and three dimensions with equal grid spacing. The expression in equation (13) has been shown in reference 4 to be equal to 1/4 and 1/6 for two and three dimensions, respectively. This restriction as shown in equation (13) is of the same magnitude as is typically used for an explicit finite difference technique for the grid Fourier number.

#### APPLICATIONS

The exponential finite difference technique will now be applied to a number of engineering problems. Unsteady heat transfer problems will be solved in one-dimensional radial coordinates, in one-dimensional Cartesian coordinates with temperature-varying thermal conductivity, and in three-dimensional Cartesian coordinates. Nonlinear equations will also be numerically solved using this method. In particular, Burger's equation and the laminar boundary

layer on a flat plate will be investigated. All applications will be compared either to exact results or to results obtained via other numerical techniques. This comparison will provide an assessment of the accuracy of the exponential finite difference method.

### One-Dimensional Heat Conduction in Cylindrical Coordinates

One-dimensional heat conduction in cylindrical coordinates will be investigated for infinite and finite heat transfer coefficient. The exact results for both cases can be found in reference 5.

For infinite heat transfer coefficient on the boundary surface the exact result is given in reference 5 as

$$\frac{T(r,t) - T_{\infty}}{T_0 - T_{\infty}} = 2 \sum_{\bar{m}=1}^{\infty} \frac{e^{-\alpha \lambda_{\bar{m}}^2 t} J_0(\lambda_{\bar{m}} r)}{(\lambda_{\bar{m}} R) J_1(\lambda_{\bar{m}} R)} \quad (14)$$

where  $\lambda_{\bar{m}} R$  is the  $\bar{m}$ th zero of

$$J_0(\lambda_{\bar{m}} R) = 0 \quad (15)$$

The results of both the exact analysis and the exponential finite difference method are shown in table I. As can be seen from the tabulated results, exponential finite difference results approach the exact solution as the number of nodes is increased or as the dimensionless time step is decreased.

When the heat transfer coefficient has a finite value at the surface, the exact solution from reference 5 is

$$\frac{T(r,t) - T_{\infty}}{T_0 - T_{\infty}} = 2B \sum_{\bar{m}=1}^{\infty} \frac{e^{-\alpha \lambda_{\bar{m}}^2 t} J_0(\lambda_{\bar{m}} r)}{(\lambda_{\bar{m}}^2 R^2 + B^2) J_0(\lambda_{\bar{m}} R)} \quad (16)$$

where  $B = hR/k$  (Biot modulus) and  $\lambda_{\bar{m}}$  (characteristics values) are given by the following equation (for cooling):

$$(\lambda_{\bar{m}} R) J_1(\lambda_{\bar{m}} R) - B J_0(\lambda_{\bar{m}} R) = 0 \quad (17)$$

The results are shown in table II for various values of the Biot modulus. As would be expected, the solution approaches the exact solution as the number of nodes increases. As the elapsed time of the solution proceeded, temperatures predicted by the exponential finite difference method approached the exact result. Also the results indicated that reducing the size of the time subinterval increased the accuracy of the method.

One last comparison will be made while investigating the exponential finite difference technique in one-dimensional cylindrical coordinates. The geometry for a cylindrical annulus is shown in figure 1 and is applied to a problem with the following initial and boundary conditions:

$$\left. \begin{aligned} T(r,0) &= 0 \\ T(R_2,t) &= 1.0 \\ \frac{\partial T}{\partial r}(R_1,t) &= 0 \end{aligned} \right\} \quad (18)$$

In reference 6 this problem was solved numerically using a characteristic-value solution. A comparison of results is shown in table III for the exponential method using the same grid spacing as in reference 6 and for the case where grid spacing is halved. The results are seen to compare quite well with the finer mesh being slightly closer to the value from reference 6 especially during the first few time steps of the solution.

#### One-Dimensional Unsteady State Conduction With Temperature-Varying Thermal Conductivity

The effect of temperature-varying thermal conductivity will now be investigated using three different numerical schemes: a pure explicit, the exponential method, and an implicit technique. The problem to be solved is illustrated in figure 2(a). The thermal conductivity is assumed to be a linear function of temperature and is shown in figure 2(b).

The exponential finite difference method will be applied first to the given problem. The following governing partial differential equation is taken from reference 7:

$$\rho C_p \frac{\partial T}{\partial t} = \frac{\partial}{\partial x} \left( k \frac{\partial T}{\partial x} \right) \quad (19)$$

Equation (19) can be changed to a simpler form by using an alternate dependent variable  $\theta$  (the Kirchoff transformation) given by

$$\theta = \frac{1}{k_R} \int_{T_R}^T k(T) dt \quad (20)$$

where  $k_R$  is the conductivity at temperature  $T_R$ , and

$$\left. \begin{aligned} \frac{\partial \theta}{\partial t} &= \frac{k}{k_R} \frac{\partial T}{\partial t} \quad \text{or} \quad \frac{\partial T}{\partial t} = \frac{k_R}{k} \frac{\partial \theta}{\partial t} \\ \frac{\partial \theta}{\partial x} &= \frac{k}{k_R} \frac{\partial T}{\partial x} \quad \text{or} \quad \frac{\partial T}{\partial x} = \frac{k_R}{k} \frac{\partial \theta}{\partial x} \end{aligned} \right\} \quad (21)$$

Substituting equations (21) into equation (19) gives

$$\frac{\rho C_p k_R}{k} \left( \frac{\partial \theta}{\partial t} \right) = \frac{\partial}{\partial x} \left( k_R \frac{\partial \theta}{\partial x} \right)$$

or

$$\frac{\rho C_p}{k} \left( \frac{\partial \theta}{\partial t} \right) = \frac{\partial^2 \theta}{\partial x^2} \quad (22)$$

Since it has been assumed that the thermal conductivity is a linear function of temperature,

$$k(T) = k_R (1 + \beta T) \quad (23)$$

Now substituting equation (23) into equation (20) results in the following:

$$\theta = \frac{1}{k_R} \int_{T_R}^T (k_R + \beta k_R T) dT$$

Direct integration yields:

$$\theta = (T - T_R) \left[ 1 + \frac{\beta}{2} (T + T_R) \right] \quad (24)$$

Equation (24) provides the relationship between the variable  $T$  and the variable  $\theta$ .

Returning to equation (22) and rearranging results in:

$$\frac{\partial \theta}{\partial t} = \frac{k}{\rho C_p} \frac{\partial^2 \theta}{\partial x^2} \quad (25)$$

Equation (25) is in a form for which the exponential finite difference method can be applied. The resulting equation in the Kirchoff variable can be shown (ref. 4) to be given by

$$\theta_i^{n+1} = \theta_i^n \exp \left\{ \frac{\Delta t}{\rho C_p (\Delta x)^2} \left[ \frac{k_i^n (\theta_{i+1}^n + \theta_{i-1}^n - 2\theta_i^n)}{\theta_i^n} \right] \right\} \quad (26)$$

Evaluating equation (24) at node  $i$  and time step  $n$  results in

$$\theta_i^n = (T_i^n - T_R) + \frac{\beta}{2} \left[ (T_i^n)^2 + T_R^2 \right] \quad (27)$$

Substitution of equation (27) into equation (26) at the appropriate time steps and nodal locations yields

$$\begin{aligned}
& (T_i^{n+1} - T_R) + \frac{\beta}{2} \left[ (T_i^{n+1})^2 - T_R^2 \right] = \left\{ (T_i^n - T_R) + \frac{\beta}{2} \left[ (T_i^n)^2 - T_R^2 \right] \right\} \\
& \times \exp \left( \gamma k_i^n \left\{ \frac{(T_{i+1}^n + T_{i-1}^n - 2T_i^n) + \frac{\beta}{2} \left[ (T_{i+1}^n)^2 + (T_{i-1}^n)^2 - 2(T_i^n)^2 \right]}{(T_i^n - T_R) + \frac{\beta}{2} \left[ (T_i^n)^2 - T_R^2 \right]} \right\} \right) \quad (28)
\end{aligned}$$

where

$$\gamma = \frac{\Delta t}{\rho C_p (\Delta x)^2}$$

If  $T_R = T_\infty = 0.0$ , equation (28) becomes

$$\begin{aligned}
& T_i^{n+1} + \frac{\beta}{2} (T_i^{n+1})^2 = \left( T_i^n + \frac{\beta}{2} T_i^n \right) \\
& \times \exp \left( \gamma k_i^n \left\{ \frac{(T_{i+1}^n + T_{i-1}^n) - 2T_i^n + \frac{\beta}{2} \left[ (T_{i+1}^n)^2 + (T_{i-1}^n)^2 - 2(T_i^n)^2 \right]}{T_i^n + \frac{\beta}{2} (T_i^n)^2} \right\} \right) \quad (29)
\end{aligned}$$

The equation for  $T_i^{n+1}$  is a quadratic with the right side of the equation that is known at time step  $n$ . Hence, define a variable,  $\kappa_i$ , such that

$$\begin{aligned}
& \kappa_i = \left[ T_i^n + \frac{\beta}{2} (T_i^n)^2 \right] \\
& \times \exp \left( \gamma k_i^n \left\{ \frac{(T_{i+1}^n + T_{i-1}^n - 2T_i^n) + \frac{\beta}{2} \left[ (T_{i+1}^n)^2 + (T_{i-1}^n)^2 - 2(T_i^n)^2 \right]}{T_i^n + \frac{\beta}{2} (T_i^n)^2} \right\} \right) \quad (30)
\end{aligned}$$

Equation (29) then becomes

$$\left( T_i^{n+1} \right)^2 + \frac{2}{\beta} T_i^{n+1} - \frac{2}{\beta} \kappa_i = 0 \quad (31)$$

Solving this and using the positive root results in

$$T_i^{n+1} = \frac{1}{\beta} \left( -1 + \sqrt{1 + 2\kappa_i\beta} \right) \quad (32)$$

where  $\beta > 0$ .

Equation (32) and equation (30) are solved using the exponential finite difference solution sequence. In this case the conductivity as well as the temperature field must be monitored on the subtime interval level. The dimensionless time step,  $\Omega$ , and the rate of conductivity change,  $\beta$ , must both be considered when choosing the step size so the solution does not become unstable. For this method, the term  $[\gamma k_i^n / (m + 1)]$  in the exponential was considered at its maximum possible value and the time step was adjusted to retain stability. This criteria was chosen so that

$$\frac{\gamma k_i^n}{m + 1} < 0.5$$

A comparison of results obtained by using a pure explicit method, a pure implicit method, and the exponential method can be found in figure 3 and table IV. Figure 3 shows the temperature field over a slab cross section. From this, it is evident that the exponential and pure explicit methods give very similar results. The implicit method predicted higher temperatures closer to the slab surface and lower temperatures at the slab centerline. In table IV the results at the slab center are shown for various elapsed times. As can be seen, all three methods agreed with each other to within a few percent.

#### Unsteady Heat Conduction in Three Dimensions

A final application of the exponential finite difference method to the diffusion equation will be for three-dimensional, unsteady heat conduction. The exponential method, a pure explicit method, and an implicit method (method of Douglas, ref. 8) will be compared to an exact solution for the problem shown in figure 4.

The exact solution to the problem illustrated in figure 4 is given in reference 9 as

$$\begin{aligned} \frac{T(x,y,z,t) - T_1}{T_0 - T_1} = & 8 \sum_{m_1=0}^{\infty} \sum_{n_1=0}^{\infty} \sum_{p_1=0}^{\infty} \left[ \frac{(-1)^{m_1+n_1+p_1}}{\left(m_1 + \frac{1}{2}\right)\left(n_1 + \frac{1}{2}\right)\left(p_1 + \frac{1}{2}\right)} \right] \\ & \times \exp \left\{ - \left[ \frac{\left(m_1 + \frac{1}{2}\right)^2}{a^2} + \frac{\left(n_1 + \frac{1}{2}\right)^2}{b^2} + \frac{\left(p_1 + \frac{1}{2}\right)^2}{c^2} \right] \pi^2 \alpha t \right\} \\ & \times \cos \left[ \left(m_1 + \frac{1}{2}\right) \frac{\pi x}{a} \right] \cos \left[ \left(n_1 + \frac{1}{2}\right) \frac{\pi y}{b} \right] \cos \left[ \left(p_1 + \frac{1}{2}\right) \frac{\pi z}{c} \right] \quad (33) \end{aligned}$$

where  $a$ ,  $b$ , and  $c$  are the widths of the cube in the  $x$ -,  $y$ -, and  $z$ -directions, respectively. Equation (33) will be used to determine how well the numerical techniques predict the temperature distribution.

The exponential finite difference technique will be investigated first. The sequence to be followed for determining the finite difference equation is the same as that presented for the earlier cases. The step-by-step procedure for this three-dimensional case consists of the following:

- (1) Linearize the partial differential equation
- (2) Assume a product solution
- (3) Separate time from spatial dependence
- (4) Solve for time dependence
- (5) Insert the appropriate spatial finite differences into exponential term that results from step 3

Based on this procedure the three-dimensional exponential finite difference equation can be shown to be the following (ref. 4):

$$T_{i,j,k}^{n+1} = T_{i,j,k}^n \exp \left[ \Omega \left( \frac{T_{i+1,j,k}^n + T_{i-1,j,k}^n - 2T_{i,j,k}^n}{T_{i,j,k}^n} + \frac{T_{i,j+1,k}^n + T_{i,j-1,k}^n - 2T_{i,j,k}^n}{T_{i,j,k}^n} + \frac{T_{i,j,k+1}^n + T_{i,j,k-1}^n - 2T_{i,j,k}^n}{T_{i,j,k}^n} \right) \right] \quad (34)$$

By using subtime intervals, equation (34) becomes

$$T_{i,j,k}^{n+1} = T_{i,j,k}^n \exp \left[ \frac{\Omega}{m+1} \sum_{p=0}^m M_{i,j,k}^{n+p/(m+1)} \right] \quad (35)$$

where  $m$  is the number of subtime intervals,  $\Omega$  is the dimensionless time step, and  $M_{i,j,k}^n$  is the dimensionless drive number given by

$$M_{i,j,k}^n = \frac{T_{i+1,j,k}^n + T_{i-1,j,k}^n - 2T_{i,j,k}^n}{T_{i,j,k}^n} + \frac{T_{i,j+1,k}^n + T_{i,j-1,k}^n - 2T_{i,j,k}^n}{T_{i,j,k}^n} + \frac{T_{i,j,k+1}^n + T_{i,j,k-1}^n - 2T_{i,j,k}^n}{T_{i,j,k}^n} \quad (36)$$

Equation (35) will be used for all interior node in figure 4. This equation, as well as those that result from the other analysis, will be modified along the insulated boundaries to account for the proper boundary conditions.

The next method to be applied to this three-dimensional case will be the pure explicit method. The finite difference equation for this method is given by following (ref. 8):

$$T_{i,j,k}^{n+1} = T_{i,j,k}^n (1 - 6\Omega) + \Omega \left( T_{i+1,j,k}^n + T_{i-1,j,k}^n + T_{i,j+1,k}^n + T_{i,j-1,k}^n + T_{i,j,k+1}^n + T_{i,j,k-1}^n \right) \quad (37)$$

where  $\Omega = (\alpha \Delta t) / (\Delta x)^2$  and  $\Delta x = \Delta y = \Delta z$ . As shown in reference 8, the dimensionless time step  $\Omega$  must be

$$\Omega \leq \frac{1}{6} \quad (38)$$

to ensure stability of the method.

The last numerical technique that will be applied is the method of Douglas (ref. 8). This method is implicit, and the spatial directions are considered sequentially in the x-, y-, and z-directions, respectively. The intermediate temperatures  $\bar{U}$  (found from the x-direction sweep) and  $\bar{V}$  (found from y-direction sweep) are used to calculate the actual temperature field variable  $T$  (found from z-direction sweep). The equations that are solved sequentially are presented as follows:

$$\frac{\bar{U}_{i,j,k} - T_{i,j,k}^n}{\alpha \Delta t} = \frac{1}{2} \delta_x^2 \left( \bar{U}_{i,j,k} + T_{i,j,k}^n \right) + \delta_y^2 \left( T_{i,j,k}^n \right) + \delta_z^2 \left( T_{i,j,k}^n \right) \quad (39)$$

$$\frac{\bar{V}_{i,j,k} - T_{i,j,k}^n}{\alpha \Delta t} = \frac{1}{2} \delta_x^2 \left( \bar{U}_{i,j,k} + T_{i,j,k}^n \right) + \frac{1}{2} \delta_y^2 \left( \bar{V}_{i,j,k} + T_{i,j,k}^n \right) + \delta_z^2 \left( T_{i,j,k}^n \right) \quad (40)$$

$$\frac{T_{i,j,k}^{n+1} - T_{i,j,k}^n}{\alpha \Delta t} = \frac{1}{2} \delta_x^2 \left( \bar{U}_{i,j,k} + T_{i,j,k}^n \right) + \frac{1}{2} \delta_y^2 \left( \bar{V}_{i,j,k} + T_{i,j,k}^n \right) + \frac{1}{2} \delta_z^2 \left( T_{i,j,k}^{n+1} + T_{i,j,k}^n \right) \quad (41)$$

where the finite difference operator in the x-direction, for example, would be

$$\delta_x^2 = \frac{(\quad)_{i+1,j,k} + (\quad)_{i-1,j,k} - 2(\quad)_{i,j,k}}{\Delta x^2} \quad (42)$$

Equations (39) to (41) must be solved successively because the variable  $\bar{U}$  is used in equation (40) to find  $\bar{V}$  and so on. Since the method operates on one

spatial direction at a time, the Thomas Algorithm can be utilized. In the case of finding the  $\bar{U}$  variable, the  $y$  and  $z$  nodal values are held constant for the  $x$ -direction sweep. This process is repeated until all  $y$  and  $z$  nodal values for the  $x$ -direction variable  $\bar{U}$  are calculated. This procedure is then repeated in a similar way for the  $\bar{V}$  variable and then finally for the actual temperature field variable.

The results from the three methods are shown in table V. As may be seen, the exponential finite difference method gave more accurate predictions for the nodal positions shown. Also in table V the standard deviation of the diagonal values are shown. The exponential method had a smaller standard deviation at both elapsed times shown in table V.

In reference 8 nine different methods to solve the diffusion equation in three dimensions were investigated. The method of Douglas was the preferred method because of its accurate results and low computer CPU time. In that study the pure explicit method required the lowest amount of CPU time with the method of Douglas requiring approximately four times as much. In the present study all three methods were run on two different mainframe computers to investigate how these three methods compared in terms of CPU time. The results are shown in table VI. All three methods were exercised for the same number of time steps. As indicated, the exponential method was approximately three times faster than the method of Douglas but still slower than the pure explicit method. From these results it could be concluded that the exponential method would have been chosen as the preferred method for overall accuracy and CPU time.

#### Viscous Burger's Equation

The viscous Burger's equation is given in reference 10 as

$$\frac{\partial U}{\partial t} + U \frac{\partial U}{\partial x} = \nu \frac{\partial^2 U}{\partial x^2} \quad (43)$$

The equation must be linearized first in order to apply the exponential method. Hence, letting  $U = A = \text{constant}$  for the nonlinear term and rearranging the equation give

$$\frac{\partial U}{\partial t} = -A \frac{\partial U}{\partial x} + \nu \frac{\partial^2 U}{\partial x^2} \quad (44)$$

Dividing by  $U$  and evaluating the resulting expression at time  $n$  at node  $i$  result in

$$\left. \frac{\partial \ln U}{\partial t} \right|_i^n = \left[ \frac{1}{U} \left( \nu \frac{\partial^2 U}{\partial x^2} - A \frac{\partial U}{\partial x} \right) \right]_i^n \quad (45)$$

The spatial and time terms are now separated so either side can be set equal to a constant  $-\kappa$

$$\left. \frac{\partial \ln U}{\partial t} \right|_i^n = -\kappa \quad (46)$$

This can be shown to be equal to

$$\frac{U_i^{n+1}}{U_i^n} = e^{-\kappa \Delta t} \quad (47)$$

Also, equation (45) can be shown to be the following (ref. 4):

$$\frac{1}{U_i^n} \left[ -U_i^n \left( \frac{U_{i+1}^n - U_{i-1}^n}{2 \Delta x} + v \left( \frac{U_{i+1}^n + U_{i-1}^n - 2U_i^n}{(\Delta x)^2} \right) \right) \right] = -\kappa \quad (48)$$

This is used to replace the exponent in equation (47)

$$U_i^{n+1} = U_i^n \exp \left\{ \frac{\Delta t v}{(\Delta x)^2} \left[ -\frac{\Delta x}{2v} (U_{i+1}^n - U_{i-1}^n) + \left( \frac{U_{i+1}^n + U_{i-1}^n - 2U_i^n}{U_i^n} \right) \right] \right\} \quad (49)$$

Equation (49) is the exponential finite difference equation for the viscous Burger's equation.

An exact steady-state solution to Burger's equation is available for the following conditions:

$$U(0,t) = U_0$$

$$U(L,t) = 0$$

The steady-state solution was given as the following (ref. 10):

$$U(x) = U_0 U_1 \left\{ \frac{1 - \exp \left[ U_1 \operatorname{Re} \left( \frac{x}{L} - 1 \right) \right]}{1 + \exp \left[ U_1 \operatorname{Re} \left( \frac{x}{L} - 1 \right) \right]} \right\}$$

where

$$\operatorname{Re}_L = \frac{U_0 L}{v} \quad (50)$$

and  $U_1$  is the solution of the following equation:

$$\frac{U_1 - 1}{U_1 + 1} = \exp \left( -U_1 \operatorname{Re}_L \right)$$

The exponential finite difference method will be now used to numerically solve the previous problem. However, for the stated conditions, a problem

arises with the portion of the velocity field is initially zero. To overcome this difficulty, a substitution will be used in which a new variable is defined such that

$$\bar{U} = U_0 - U$$

Burger's equation then becomes

$$\frac{\partial \bar{U}}{\partial t} = (\bar{U} - U_0) \frac{\partial \bar{U}}{\partial x} + \nu \frac{\partial^2 \bar{U}}{\partial x^2} \quad (51)$$

with the following imposed conditions if  $U_0 = 1$ :

$$\left. \begin{aligned} \bar{U}(0,t) &= 0 \\ \bar{U}(L,t) &= U_0 \end{aligned} \right\} \quad (52)$$

The same method of separation of variables must be performed on the  $\bar{U}$  variable in equation (51). The problem is now solved for the  $\bar{U}$  variable and the substitution shown above is then made to find the  $U$  variable. The exponential finite difference equation for  $\bar{U}$  can be shown to be (ref. 4):

$$\bar{U}_i^{n+1} = \bar{U}_i^n \exp \left[ \frac{\Delta t \nu}{(\Delta x)^2} \left\{ \frac{-\Delta x}{2\nu} \left[ \frac{(1 - \bar{U}_i^n)(\bar{U}_{i+1}^n - \bar{U}_{i-1}^n)}{\bar{U}_i^n} \right] + \frac{(\bar{U}_{i+1}^n + \bar{U}_{i-1}^n - 2\bar{U}_i^n)}{\bar{U}_i^n} \right\} \right] \quad (53)$$

The results obtained by applying equation (53) and the conditions in equations (52) are compared to the steady-state exact results of equation (50) and are shown in figure 5. The results from the exponential method were nearly the same as those from the exact method.

Another application of Burger's equation was done to investigate the effect of the diffusion term. The results for the variation of  $\nu$  over four orders of magnitude are shown in figure 6 for the same instant in time. At the two lower  $\nu$  values, the total range of the field variable takes place over a small number of nodal positions. A better approximation could be made for these cases by using a finer grid. A comparison of the exponential and a pure explicit finite differencing schemes for Burger's equation are shown in figure 7. As can be seen from figure 7, the number of nodes used can have a large effect on the predicted velocity field. The pure explicit techniques can have large oscillations and predict physically impossible results. As the number of nodes are increased and the time step decreased, the two solutions give similar results.

## Laminar Boundary Layer on a Flat Plate

The last application to be investigated will be for the development of a laminar boundary layer on a flat plate (fig. 8). In reference 9 the steady-state formulation is given in terms of the following three partial differential equations:

Continuity:

$$U \frac{\partial U}{\partial x} + V \frac{\partial V}{\partial y} = 0 \quad (54)$$

Momentum:

$$U \frac{\partial U}{\partial x} + V \frac{\partial U}{\partial y} = \nu \frac{\partial^2 U}{\partial y^2} \quad (55)$$

Energy:

$$U \frac{\partial T}{\partial x} + V \frac{\partial T}{\partial y} = \alpha \frac{\partial^2 T}{\partial y^2} \quad (56)$$

with the following boundary conditions:

$$\left. \begin{aligned} U(x,0) &= 0 & U(0,y) &= U_0 \\ V(x,0) &= 0 & V(x,L) &= 0 \\ T(x,0) &= 0 & T(0,y) &= T_0 \end{aligned} \right\} \quad (57)$$

where  $\nu$  and  $\alpha$  are the momentum and thermal diffusivities, respectively.

Equations (55) and (56) can be solved by using the method presented for the viscous Burger's equation. The only difference is that the solution will march in the  $x$ -direction instead of time. The results from the separation of variables for equations (55) and (56) were found to be (ref. 4)

$$U_j^{i+1} = U_j^i \exp \left( \frac{\Delta x}{U_j^i} \left\{ -\frac{V_j^i}{U_j^i} \left( \frac{U_{j+1}^i - U_{j-1}^i}{2 \Delta y} \right) + \frac{\nu}{U_j^i} \left[ \frac{U_{j+1}^i + U_{j-1}^i - 2U_j^i}{(\Delta y)^2} \right] \right\} \right) \quad (58)$$

$$T_j^{i+1} = T_j^i \exp \left( \frac{\Delta x}{T_j^i} \left\{ \frac{-V_j^i}{U_j^i} \left( \frac{T_{j+1}^i - T_{j-1}^i}{2 \Delta y} \right) + \frac{\alpha}{U_j^i} \left[ \frac{T_{j+1}^i + T_{j-1}^i - 2T_j^i}{(\Delta y)^2} \right] \right\} \right) \quad (59)$$

The continuity equation is written as (ref. 10)

$$V_j^{i+1} = V_{j-1}^{i+1} - \frac{\Delta y}{2 \Delta x} \left( U_j^{i+1} - U_j^i + U_{j-1}^{i+1} - U_{j-1}^i \right) \quad (60)$$

Equations (58) and (59) are first solved using a spatial subincrement as was done for the cases when time was the marching direction of the solution. After this, the continuity equation (eq. (60)) is solved.

The results of this application are shown in figure 9 for a Prandtl number equal to 0.72. The thermal boundary layer was outside the velocity boundary layer, as would be expected. The results with the Prandtl number equal to 0.72 were compared to the exact solution as presented in reference 9. A downstream position was chosen and the results are compared in table VII. The exponential method results were in good agreement with the exact results.

#### CONCLUDING REMARKS

In conclusion, an exponential finite difference technique has been extended to other coordinate systems and expanded to model problems in two and three dimensions. The method has direct application to linear partial differential equations such as the diffusion equation and can be extended to solve nonlinear equations. The method is presented as an alternative method for solving a wide range of engineering problems.

The method was applied to a variety of heat conduction and fluid flow problems. It was found that the results predicted by the exponential finite difference algorithm for the cases presented in this study demonstrated that

1. Field variable was predicted with a higher degree of accuracy than other numerical techniques where exact solutions exist.
2. The method can be applied to linear and nonlinear partial differential equations with dependent variables that can be separated.
3. When the exponential method is applied to the diffusion equation, the stability of the method is the same as that of pure explicit methods, where the subtime interval step size determines the stability.

#### REFERENCES

1. Bhattacharya, M.: An Explicit Conditionally Stable Finite Difference Equation for Heat Conduction Problems. *Int. J. Numer. Methods Eng.*, vol. 21, no. 2, Feb. 1987, pp. 239-265.
2. Bhattacharya, M.C.: A New Improved Finite Difference Equation For Heat Transfer During Transient Change. *Appl. Math. Modelling*, vol. 10, no. 1, Feb. 1986, pp. 68-70.
3. Bhattacharya, M.C.; and Davies, M.G.: The Comparative Performance of Some Finite Difference Equations for Transient Heat Conduction. *Int. J. Numer. Methods Eng.*, vol. 24, no. 7, July 1987, pp. 1317-1331.
4. Handschuh, R.F.: An Exponential Finite Difference Technique for Solving Partial Differential Equations. NASA TM-89874, Master of Science Thesis, University of Toledo, 1987.

5. Arpaci, V.S.: Conduction Heat Transfer. Addison-Wesley, 1966.
6. Carnahan, B.; Luther, H.A.; and Wilkes, J.O.: Applied Numerical Methods. John Wiley & Sons, 1969.
7. Carslaw, H.S.; and Jaeger, J.C.: Conduction of Heat in Solids. 2nd ed., Clarendon Press, Oxford, 1959.
8. Thibault, J.: Comparison of Nine Three-Dimensional Numerical Methods for the Solution of the Heat Diffusion Equation. Numerical Heat Transfer, vol. 8, no. 3, 1985, pp. 281-298.
9. Bird, R.B.; Stewart, W.E.; and Lightfoot, E.N.: Transport Phenomena. John Wiley & Sons, 1960.
10. Anderson, D.A.; Tannehill, J.C.; and Pletcher, R.H: Computational Fluid Mechanics and Heat Transfer, McGraw-Hill, 1984.

TABLE I. - COMPARISON OF RESULTS FOR DIFFERENT DIMENSIONLESS TIME STEPS FOR ONE-DIMENSIONAL HEAT TRANSFER IN CYLINDRICAL COORDINATES WITH INFINITE HEAT TRANSFER COEFFICIENT AT THE SURFACE

[Initial and boundary conditions are the following:  $h \rightarrow \infty$ ;  $T(r,0) = 1.0$ ;  $T(R,t) = 0.0$  for  $t > 0$ ;  $\Omega = (\alpha \Delta t)/(\Delta r)^2$ ;  $\alpha = 1.0 \text{ m}^2/\text{s}$ ;  $N = \text{number of nodes}$ ;  $m = \text{number of subtime intervals}$ .]

Time, t, s	Distance from surface, r, m	Exponential finite difference results, °C				Exact analysis (ref. 5), °C
		N = 11, m = 4, $\Omega = 1.0$	N = 21, m = 9, $\Omega = 1.0$	N = 21, m = 9, $\Omega = 2.0$	N = 21, m = 9, $\Omega = 5.0$	
0.1	0.1	0.127004	0.126768	0.126819	0.127059	0.126669
.1	1.0	.862431	.852204	.853083	.855980	.848368
.5	.1	.011959	.011671	.011680	.011715	.011582
.5	1.0	.094334	.090309	.090379	.090652	.089895
0.5	---	Total 50 steps $\frac{\Omega}{m+1} = 0.2$	Total 200 steps $\frac{\Omega}{m+1} = 0.1$	Total 100 steps $\frac{\Omega}{m+1} = 0.2$	Total 40 steps $\frac{\Omega}{m+1} = 0.5$	-----

TABLE II. - FINITE HEAT TRANSFER COEFFICIENT CYLINDRICAL COORDINATES  
[ $T(r,0) = 1.0$ ,  $T_{\infty} = 0$ ,  $\Omega = (\alpha \Delta t)/(\Delta r)^2$ .]

Time, t, s	Biot modulus	Spatial coordinate, r, m	Exact analysis (ref. 5), °C	Exponential finite difference results, °C		
				N = 11, m = 4, $\Omega = 1.0$	N = 21, m = 9, $\Omega = 5.0$	N = 21, m = 9, $\Omega = 1.0$
0.1	1	1	0.6846	0.7073	0.6978	0.6962
		0	.9768	.9814	.9797	.9785
.2	1	1	.5702	.5976	.5857	.5841
		0	.8702	.8852	.8780	.8767
.4	1	1	.4132	.4441	.4303	.4285
		0	.6420	.6698	.6563	.6548
.1	2	1	.5009	.5285	.5199	.5150
		0	.9594	.9670	.9643	.9621

Time, t, s	Biot modulus	Spatial coordinate, r, m	Exact analysis (ref. 5), °C	Exponential finite difference results, °C		
				N = 11, m = 4, $\Omega = 1.0$	N = 21, m = 9, $\Omega = 2.5$	N = 21, m = 9, $\Omega = 1.0$
0.1	5	1	0.2558	0.2777	0.2669	0.2669
		0	.9265	.9385	.9313	.9306

TABLE III. - COMPARISON OF EXPONENTIAL FINITE DIFFERENCE METHOD IN ONE-DIMENSIONAL CYLINDRICAL COORDINATES TO THE RESULTS OF REFERENCE 6

[ $\alpha = 1.0 \text{ ft}^2/\text{s}$ ;  $\Delta t = 1.0 \text{ s}$ ;  $(\alpha \Delta t)/\Delta r^2 = 1.0$ ;  $N = \text{number of nodes}$ ;  $m = \text{number of subintervals}$ .]

Time, $t$ , s	Radial length, $R$ , in.	Results from reference 6	Exponential finite difference results, °F	
			$N = 10$ , $m = 4$ , $\Omega = 1.0$	$N = 19$ , $m = 8$ , $\Omega = 1.0$
5	18	0.77220	0.773094	0.772922
	10	.01449	.011353	.011951
10	18	.84661	.846719	.846811
	10	.11595	.112112	.113523
30	18	.93546	.935278	.935521
	10	.57722	.575979	.578198
90	18	.99370	.993686	.993776
	10	.95872	.958596	.959245

TABLE IV. - COMPARISON OF EXPONENTIAL, PURE-EXPLICIT, AND IMPLICIT FINITE DIFFERENCE METHODS FOR ONE-DIMENSIONAL, UNSTEADY HEAT TRANSFER WITH TEMPERATURE-VARYING THERMAL CONDUCTIVITY

[Temperature shown is at center of slab;  $K(T) = 1.0 + \beta(T)$ ;  $\beta = 0.01$ .]

Time, $t$ , s	Temperature, °C		
	Exponential finite difference ( $N = 11$ , $m = 4$ , $\Omega = 0.5$ , $\Delta t = 0.005 \text{ s}$ )	Pure explicit ( $N = 11$ , $\Omega = 0.25$ , $\Delta t = 0.0025 \text{ s}$ )	Implicit ( $\Omega = 1.0$ , $\Delta t = 0.01 \text{ s}$ )
0.01	98.15998	100.00000	94.35768
.02	88.87177	89.21321	85.90591
.05	61.30161	60.09306	61.31385
.1	34.37147	33.41929	35.37178

TABLE V. - COMPARISON OF THREE DIFFERENT, THREE-DIMENSIONAL UNSTEADY STATE HEAT TRANSFER SOLUTIONS

$$T(x, y, z, 0) = 1.0; T(x, y, L, t) = T(L, y, z, t) = 0; \frac{\partial T}{\partial x}(x, y, z, t) = \frac{\partial T}{\partial y}(x, y, 0, t) = \frac{\partial T}{\partial z}(x, y, 0, t) = 0; N = \text{number of nodes}$$

in x-, y-, and z-directions;  $\Omega = (\alpha \Delta t) / (\Delta x)^2$ ;  $\Delta x = \Delta y = \Delta z$ .

Elapsed time, s	Position from center along diagonal, x = y = z	Exact analysis results, °C	Exponential finite difference results, °C		Accuracy, percent	Pure explicit finite difference results, °C		Accuracy, percent	Method of Douglas finite difference results, °C	Accuracy, percent		
			Exponential finite difference results, °C	Accuracy, percent		Pure explicit finite difference results, °C	Accuracy, percent					
0.09	0.0	0.893490	0.892237	0.14	N = 11, m = 4, $\Omega = 0.75$	0.889437	N = 11, $\Omega = 0.15$	0.886760	N = 11, $\Omega = 0.15$	0.75		
	.5	.440712	.440650	.014		.435058		1.28			.439665	.24
	.9	.006491	.006484	.11		.006319		2.65			.006510	-.29
.15	0.0	.645469	.645209	.04	N = 11, m = 4, $\Omega = 0.75$	.640025	N = 11, $\Omega = 0.15$	.641484	N = 11, $\Omega = 0.15$	.62		
	.5	.253065	.253286	-.09		.250102		1.17			.252641	.17
	.9	.003015	.003022	-.23		.002970		1.49			.003023	-.27

Elapsed time, s	Exponential finite difference results, °C		Standard deviation along diagonal <sup>a</sup>	Pure explicit finite difference results, °C		Standard deviation along diagonal <sup>a</sup>	Method of Douglas finite difference results, °C
	Exponential finite difference results, °C	Accuracy, percent		Pure explicit finite difference results, °C	Accuracy, percent		
0.09 .15	7.24x10 <sup>-4</sup>	0.14	Standard deviation along diagonal <sup>a</sup>	4.07x10 <sup>-3</sup>	1.28	Standard deviation along diagonal <sup>a</sup>	3.65x10 <sup>-3</sup> 2.01x10 <sup>-3</sup>
	1.54x10 <sup>-4</sup>	.11		3.50x10 <sup>-3</sup>	2.65		

$$^a \text{Standard deviation} = \sqrt{\frac{1}{N} \sum_{i=1}^N (T_{e_i} - T_{c_i})^2}$$

where  $T_{e_i}$  is the exact result at the  $i$ th node,  $T_{c_i}$  is the calculated result at the  $i$ th node, and  $N$  is the number of nodes along the diagonal.

TABLE VI. - COMPARISON OF CPU TIME ON TWO DIFFERENT MAINFRAMES FOR THREE DIFFERENT THREE-DIMENSIONAL FINITE DIFFERENCE METHODS  
 [One-hundred time steps for each method.]

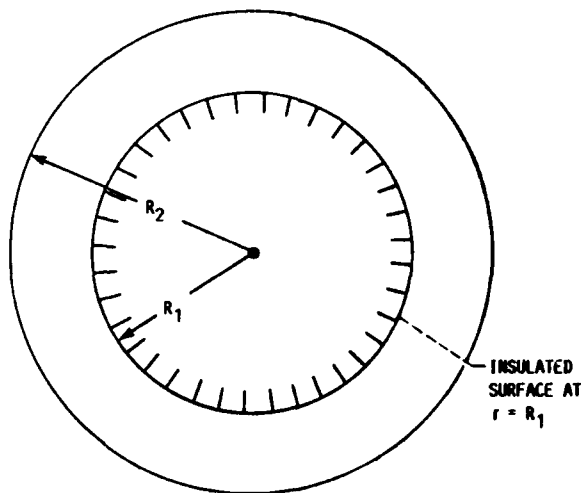
Computer	Exponential method, <sup>a</sup> s	Method of Douglas, s	Pure explicit method, s
CRAY-XMP	0.2778	0.955	0.0627
IBM-3033	5.4	12.6	1.8

<sup>a</sup>Based on the total number of subtime intervals equal to 100.

TABLE VII. - COMPARISON OF EXPONENTIAL FINITE DIFFERENCE METHOD TO EXACT RESULTS OF BOUNDARY LAYER EQUATION FROM REFERENCE 9 FOR THE VELOCITY PROFILE AT ONE DOWNSTREAM LOCATION

[Distance downstream  $x = 500$  cm,  
 $\nu = 0.0072$  cm<sup>2</sup>/s.]

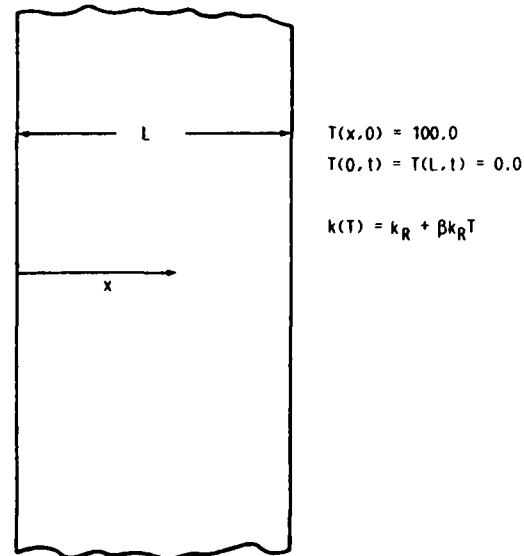
Distance perpendicular to plate, y, cm	Exact result (ref. 9)	Exponential method result (N = 21, m = 8)
1	0.17	0.17428
2	.34	.34643
3	.51	.51020
4	.65	.65658
5	.78	.77684
6	.87	.86636
7	.93	.92638
8	.96	.96265



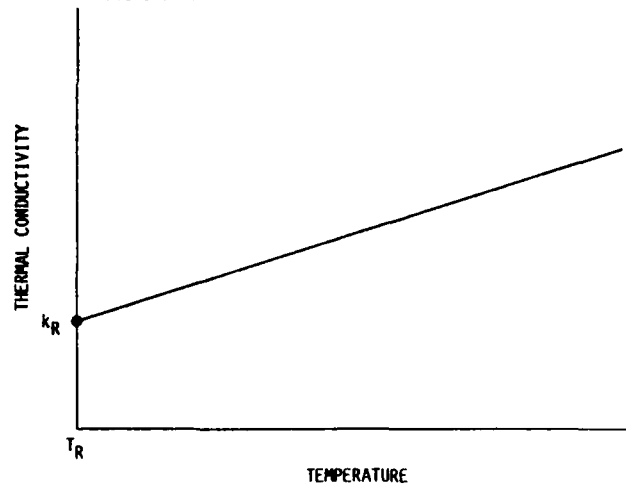
INITIAL CONDITION:  $T(r, 0) = 0$   
 BOUNDARY CONDITIONS:  $T(R_2, t) = 1.0$

$$\frac{\partial T}{\partial r}(R_1, t) = 0$$

FIGURE 1. - PROBLEM CONDITIONS FOR COMPARISON OF EXPONENTIAL FINITE DIFFERENCE TECHNIQUE TO CHARACTERISTIC PROBLEM SOLUTION.  $R_1 = 10.0$  IN.,  $R_2 = 19.0$  IN.



(A) ONE-DIMENSIONAL PROBLEM WITH VARYING THERMAL CONDUCTIVITY.



(B) LINEAR RELATIONSHIP BETWEEN CONDUCTIVITY AND TEMPERATURE.

FIGURE 2. - SKETCHES SHOWING PROBLEM STATEMENT FOR TEMPERATURE-VARYING THERMAL CONDUCTIVITY.

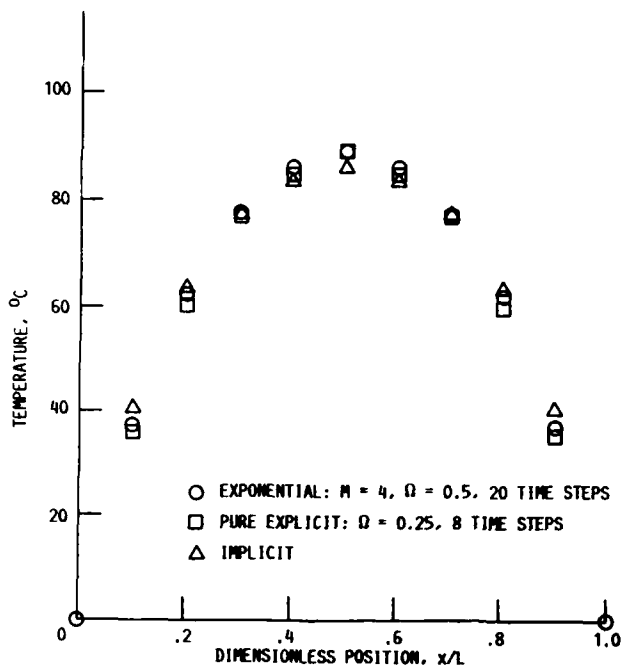


FIGURE 3. - COMPARISON OF METHODS FOR TEMPERATURE-VARYING CONDUCTIVITY, SHOWING TEMPERATURE FIELD AT  $t = 0.02$  s.  $k(T) = k_R(1 + \beta T)$  WHERE  $k_R = 1.0, \beta = 0.01, T(x,0) = 100,$  AND  $T(0,t) = T(L,t) = 0; \alpha = 1.$

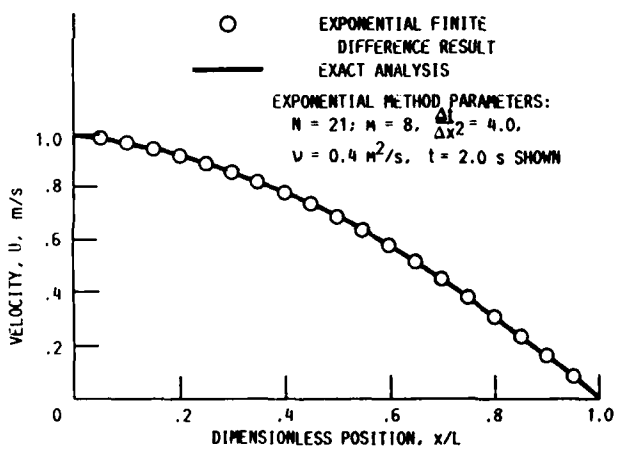
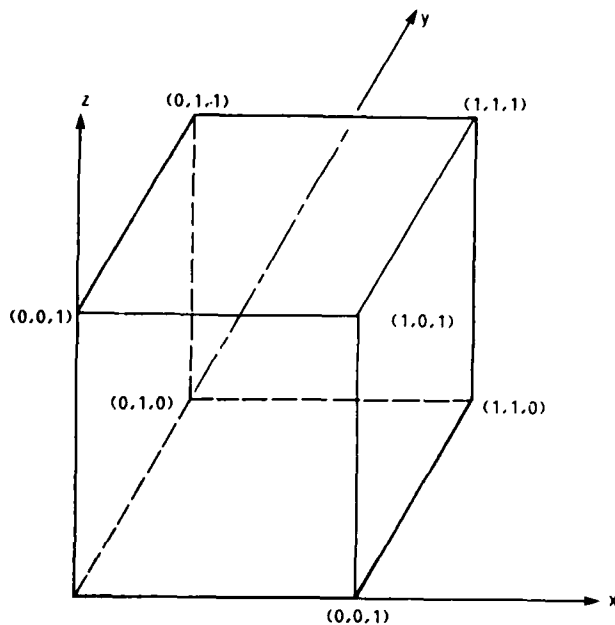


FIGURE 5. - COMPARISON OF STEADY STATE SOLUTIONS COMPARING THE EXACT RESULTS TO THE EXPONENTIAL FINITE DIFFERENCE SOLUTION  $U(0,t) = 1.0; U(L,t) = 0.0.$



INITIAL CONDITION:  $T(x,y,z,0) = T_0 = 1$

BOUNDARY CONDITIONS:  $t > 0$

$$\frac{\partial T}{\partial x}(0,y,z,t) = \frac{\partial T}{\partial y}(x,0,z,t) = \frac{\partial T}{\partial z}(x,y,0,t) = 0$$

$$T(1,y,z,t) = T(x,1,z,t) = T(x,y,1,t) = 0$$

FIGURE 4. - BOUNDARY AND INITIAL CONDITIONS FOR THREE-DIMENSIONAL UNSTEADY STATE CONDUCTION HEAT TRANSFER.

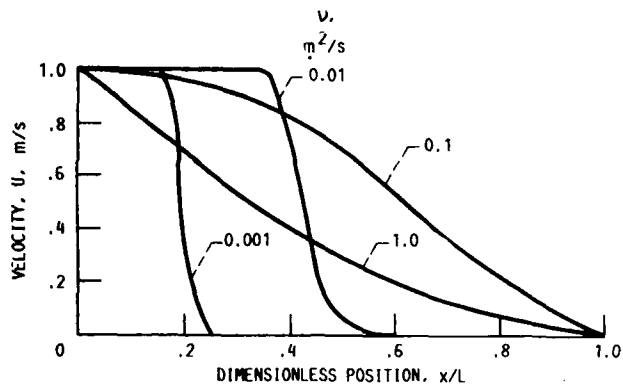


FIGURE 6. - EXPONENTIAL FINITE DIFFERENCE RESULTS FOR VARYING KINEMATIC VISCOSITY. ALL VELOCITIES ARE SHOWN FOR  $N = 21, m = 8, \Delta t / \Delta x^2 = 4.0, t = 1.0 \text{ s}, U(0,t) = 1.0, U(L,t) = 0.0.$

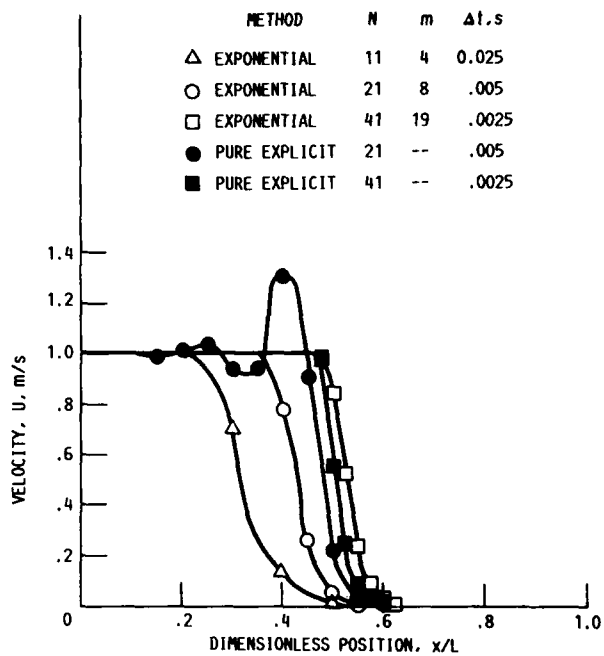


FIGURE 7. - COMPARISON OF EXPONENTIAL AND PURE EXPLICIT FINITE DIFFERENCE METHODS. ALL RESULTS SHOWN FOR  $v = 0.01 \text{ m}^2/\text{s}$ ,  $t = 1.0 \text{ s}$ ,  $U(0, t) = 1.0$ , AND  $U(L, t) = 0.0$ .

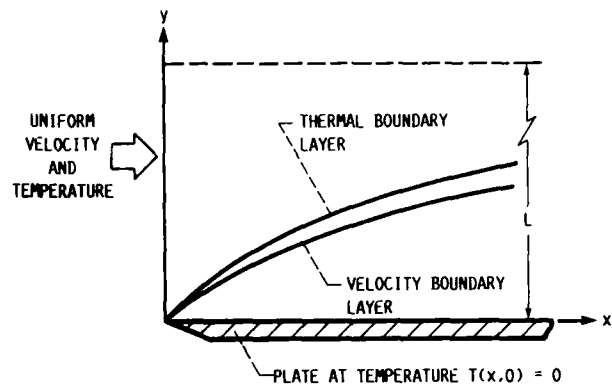


FIGURE 8. - BOUNDARY LAYER DEVELOPMENT ALONG A COOLED FLAT PLATE. CONDITIONS:  $U(x, 0) = 0$ ,  $V(x, 0) = 0$ ,  $V(x, L) = 0$ ,  $U(0, y) = 1.0$ ,  $T(0, y) = 1.0$ .

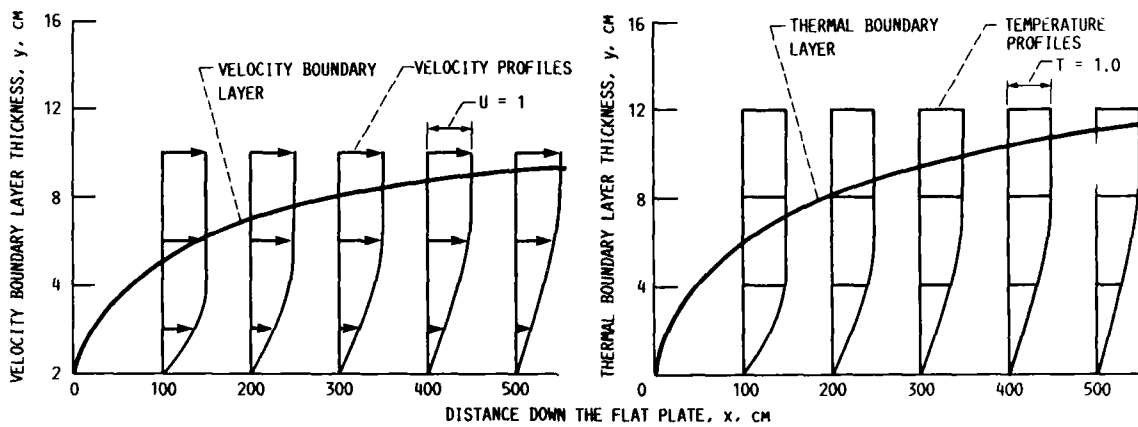


FIGURE 9. - EXPONENTIAL FINITE DIFFERENCE RESULTS FOR BOUNDARY LAYER EQUATIONS WITH CONDITIONS  $U(0, y) = 1.0$ ,  $U(x, 0) = 0$ ,  $V(x, 0) = 0$ ,  $V(x, L) = 0$ ,  $T(x, 0) = 0.0$ ,  $T(0, y) = 1.0$ ;  $v = 0.0072 \text{ cm}^2/\text{s}$ ;  $\alpha = 0.01 \text{ cm}^2/\text{s}$ .



# Report Documentation Page

1. Report No. NASA TM-100939 AVSCOM TM-88-C-004		2. Government Accession No.		3. Recipient's Catalog No.	
4. Title and Subtitle Applications of an Exponential Finite Difference Technique				5. Report Date July 1988	
				6. Performing Organization Code	
7. Author(s) Robert F. Handschuh and Theo G. Keith, Jr.				8. Performing Organization Report No. E-4006	
				10. Work Unit No. 505-63-51	
9. Performing Organization Name and Address NASA Lewis Research Center Cleveland, Ohio 44135-3191 and Propulsion Directorate U.S. Army Aviation Research and Technology Activity—AVSCOM Cleveland, Ohio 44135-3127				11. Contract or Grant No.	
				13. Type of Report and Period Covered Technical Memorandum	
				14. Sponsoring Agency Code	
12. Sponsoring Agency Name and Address National Aeronautics and Space Administration Washington, D.C. 20546-0001 and U.S. Army Aviation Systems Command St. Louis, Mo. 63120-1798					
15. Supplementary Notes Robert F. Handschuh, Propulsion Directorate, U.S. Army Aviation Research and Technology Activity—AVSCOM; Theo G. Keith, Jr., Dept. of Mechanical Engineering, University of Toledo, Toledo, Ohio 43606.					
16. Abstract An exponential finite difference scheme first presented by Bhattacharya for one-dimensional unsteady heat conduction problems in Cartesian coordinates has been extended. The finite difference algorithm developed was used to solve the unsteady diffusion equation in one-dimensional cylindrical coordinates and was applied to two- and three-dimensional conduction problems in Cartesian coordinates. Heat conduction involving variable thermal conductivity was also investigated. The method was used to solve nonlinear partial differential equations in one- (Burger's equation) and two- (boundary layer equations) dimensional Cartesian coordinates. Predicted results are compared to exact solutions where available or to results obtained by other numerical methods.					
17. Key Words (Suggested by Author(s)) Finite difference Exponential finite difference; numerical methods Heat transfer			18. Distribution Statement Unclassified - Unlimited Subject Category 37		
19. Security Classif. (of this report) Unclassified		20. Security Classif. (of this page) Unclassified		21. No of pages 28	22. Price* A03